ACS OMEGA

http://pubs.acs.org/journal/acsodf

Article

Preparation of Chitosan-Modified Bentonite and Its Adsorption Performance on Tetracycline

Xuebai Guo, Zhenjun Wu,* Zelong Wang, Fangfang Lin, Penghui Li, and Jiaxin Liu

Cite This: *ACS Omega* 2023, 8, 19455−19463

Read Online

ACCESS | Metrics & More | Article Recommendations

ABSTRACT: In this study, chitosan-modified bentonite was synthesized using the coprecipitation method. When the Na_2CO_3 content was 4% (weight of soil) and the mass ratio of chitosan to bentonite was 1:5, the adsorption performance of the chitosan/bentonite composite was best. The adsorbent was characterized by scanning electron microscopy, X-ray diffraction, Fourier transform infrared spectroscopy, and Brunauer−Emmett−Teller measurement. Various characterization results demonstrate that chitosan successfully entered the bentonite interlayer and increased layer spacing but did not modify bentonite's laminar mesoporous structure, and the $-CH_3$ and $-CH_2$ groups of chitosan appeared on chitosan-modified bentonite. Tetracycline was used as the target pollutant in the static adsorption experiment. The adsorption capacity was 19.32 mg/g under optimal conditions. The adsorption process was more consistent with the Freundlich model and the pseudo-second-order kinetic model, indicating that it was a nonmonolayer chemisorption process. The adsorption process is a spontaneous, endothermic, entropy-increasing process, according to thermodynamic characteristics.

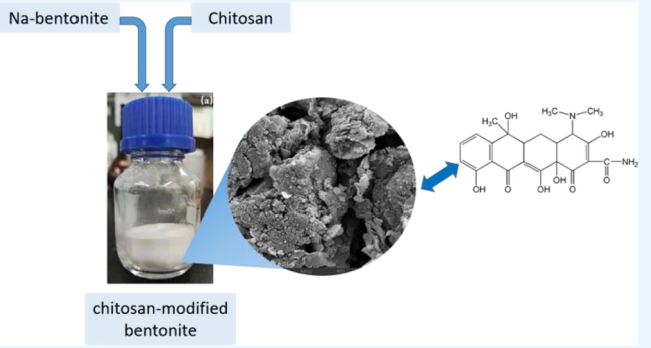

1. INTRODUCTION

With the widespread production and use of antibiotics, antibiotics in the water environment have become an emerging form of organic pollution.[1] Tetracycline (TC) is a broad-spectrum antibiotic with a polycyclic tetraphenyl carboxamide structure that is widely used in livestock and aquaculture, but its extensive use and misuse not only causes cytotoxicity to plants and animals but also leads to the spread of resistance genes and even threatens human health.[2] In recent years, researchers have found different concentrations of TC in domestic sewage and industrial wastewater.[3,4] Some studies have reported that the TC content in pharmaceutical wastewater has reached 100−500 mg/L.[5] If the treatment of TC wastewater is not complete, it will lead to an increase in residues in the environment year by year, posing a great threat to human health and the ecological environment.[6] Therefore, the removal of TC from the aqueous environment is necessary and urgent.

By comparing various treatment methods, the adsorption method has the advantages of easy operation and high removal rates and has a wide application prospect. At the same time, the adsorbent can be recycled and regenerated, which reduces the cost of wastewater treatment.[7] The commonly used adsorbents for treating TC wastewater are activated carbon,[8] MOFs,[9] bentonite,[10] biochar,[11] nanotubes,[12] metal oxides,[13] etc. Activated carbon has good adsorption effect and is widely used, but its cost is high and it is easy to lose. MOFs have the advantages of a large specific surface area and high porosity, but their preparation process is complicated and the cost is high.[14]

Bentonite is a common and inexpensive clay mineral that also serves as an environmentally friendly adsorbent.[15] It has some outstanding adsorption properties, including mesoporous structure, negatively charged surface, specific surface area, hydration, swelling, high cation exchange capacity, and chemical stability. As a result, bentonite was commonly used as an adsorbent for TC removal.[10] Natural bentonite is extremely hydrophilic and easily combines with water molecules, making organic substances on its surface difficult to diffuse and adsorb. Organic modification can improve its adsorption performance on TC by increasing its lipophilic hydrophobicity. However, the application of bentonite has drawbacks such as low adsorption efficiency, lack of selectivity, and low binding coefficients.[16]

Received: February 4, 2023
Accepted: May 4, 2023
Published: May 21, 2023

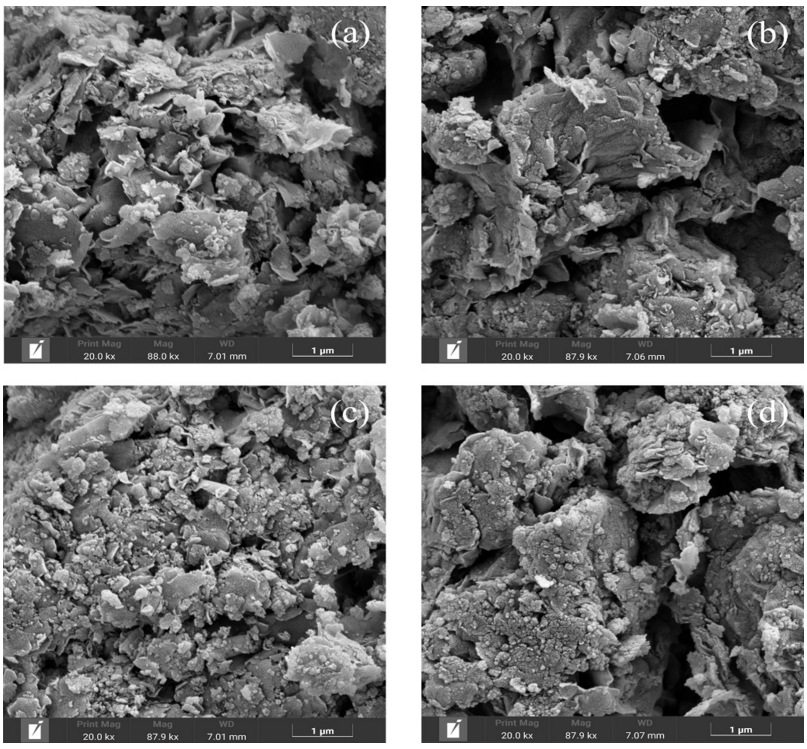

Figure 1. Scanning electron microscopy (SEM) of sodium-modified bentonite (a, c) and CS-modified bentonite (b, d).

Moreover, bentonite is easy to modify, through organic modification its hydrophilicity can be overcome, and has poor adsorption performance of organic pollutants,[17] so this study used bentonite as an adsorbent for TC. Modified bentonite not only has better adsorption performance but also can enhance the hydrophobicity of bentonite, reducing the difficulty of solid−liquid separation after adsorption, which is conducive to the regeneration of bentonite.[18] The commonly used modification methods are activation modification,[19] sodium modification,[20] and organic modification.[21] At present, the modification of bentonite has been relatively well developed, but because bentonite is hydrophilic, it is not conducive to the diffusion and adsorption of organic substances on its surface.[22] Furthermore, the difficulty of solid−liquid separation after adsorption limits its practical application. Organic modification can increase the lipophilic hydrophobicity of bentonite, which facilitates TC adsorption.[23]

Chitosan (CS) is a natural polysaccharide chitin that is used to remove part of the acetyl product and is widely used in medical, environmental protection, textile, and other industries.[24] CS is frequently used in adsorption studies due to its outstanding properties, which include minimal toxicity, biodegradability, an abundance of functional groups, and an elevated probability of interaction with binding sites.[25] CS can form stable chelates with heavy metal ions through $-NH_2$ and −OH in the molecule and can also adsorb heavy metals and organic pollutants through hydrogen bonding. Therefore, it can be widely used in wastewater treatment.[26]

CS has low chemical stability and mechanical properties, which is easily soluble in acidic solutions. This drawback limits its application as an adsorbent at low pH. Therefore, CS is usually immobilized with low-cost materials such as bentonite. The use of CS in modified bentonite can not only improve the adsorption performance of bentonite on TC but also enhance hydrophobicity and reduce the difficulty of solid−liquid separation after adsorption,[27] which has a broad application prospect. The CS/bentonite composites were applied on the adsorption of various pollutants in solution, such as heavy metals,[28] nutrients,[29] and dyes.[30] However, few studies have been carried out on antibiotic adsorption.

2. RESULTS AND DISCUSSION

2.1. Characterizations of the Adsorbents. The morphology of modified bentonite is shown in Figure 1, which shows the SEM images of bentonite that has been modified with sodium and CS, respectively. Figure 1a,b shows that sodium-modified bentonite and CS-modified bentonite both have lamellar structures, demonstrating that CS modification did not alter bentonite's fundamental structure. Figure 1c,d can be compared, and it can be seen that the surface of the CS-modified bentonite is looser. This is because CS entered between the bentonite layers, increasing the layer spacing.[31]

Figure 2 shows the XRD spectra of sodium-modified bentonite, CS-modified bentonite (1:5), and calcium-based bentonite. The XRD spectra of calcium-based bentonite, sodium-modified bentonite, and CS-modified bentonite showed essentially the same peak shapes for the three adsorbent materials without significant changes, indicating that the sodium-modified and CS-modified did not destroy the interlayered structure of bentonite.[32] However, the position of the "001" diffraction peak was shifted, indicating that the molecular layer spacing of bentonite was changed after sodium modification and CS modification.[33]

The (001) diffraction peaks of the three adsorbents appeared at 5.92°, 7.08°, and 5.77°, respectively. The spacing of $d(001)$ can be calculated by Bragg's law.[16] It is expressed as in eq 1:

$$2d \sin\theta = n\lambda \quad (1)$$

https://doi.org/10.1021/acsomega.3c00745
ACS Omega 2023, 8, 19455−19463

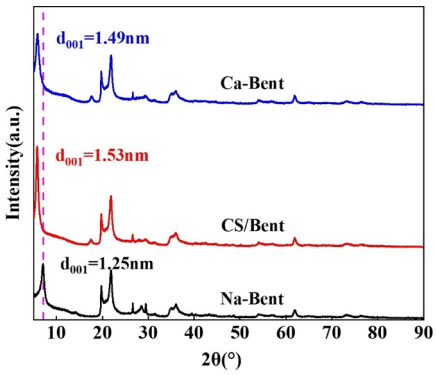

Figure 2. X-ray powder diffraction (XRD) diagram of sodium-modified bentonite, CS-modified bentonite (1:5), and calcium bentonite.

where d is the spacing between the planes, θ is the diffraction angle between the incident and reflected X rays, n represents the order of the reflection, and λ represent the wavelength of the X-ray (~0.15418 nm). The layer spacing of calcium bentonite, sodium-modified bentonite, and CS-modified bentonite was 1.49, 1.25, and 1.53 nm, respectively. The layer spacing of the sodium-modified bentonite is significantly smaller than that of the calcium-based bentonite, indicating that Na^+ has successfully entered the interlayer of bentonite and replaced Ca^{2+}, resulting in the reduction of the layer spacing.[34] The layer spacing of sodium-modified bentonite modified by CS increased significantly, which proves that CS successfully entered the interlayer of sodium-modified bentonite and increased the layer spacing.[35] The XRD spectra shown above reflect the effectiveness of this experiment applying the CS modification approach.

The FTIR spectra of CS, sodium-modified bentonite, and CS-modified bentonite are shown in Figure 3. Bentonite

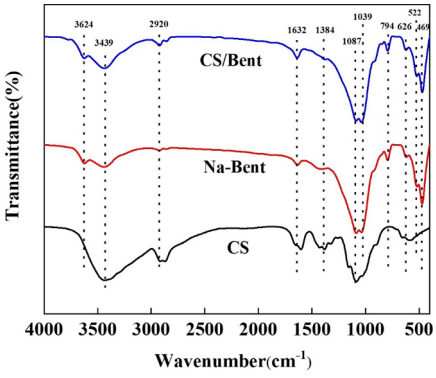

Figure 3. Fourier transform infrared spectroscopy (FTIR) diagram of CS, sodium-modified bentonite, and CS-modified bentonite.

displays peaks at 3624 cm^{-1} (Al−OH and Si−OH stretching vibration), 1632 cm^{-1} (H−O−H bending vibration), 626 cm^{-1} (Al−O stretching), 794 cm^{-1} (Al−OH vibration), and 522 and 469 cm^{-1} (Si−O bending), which are consistent with previous studies.[28] The FTIR spectrum of CS exhibits characteristic peaks at 3439 cm^{-1} (O−H and N−H stretching vibration), 2920 cm^{-1} (C−H symmetric stretching), 1632 cm^{-1} (amide II band stretching), and 1087 and 1039 cm^{-1} (−C−O stretching vibration in −C−OH).[33] The spectrum of the CS/bentonite composite reveals a characteristic band at 3439 cm^{-1}, which is because of hydrogen bond formation between functional groups of CS (N−H and O−H groups) and O−H groups in bentonite.[16] These results indicate that CS has been doped in bentonite; moreover, the CS/bentonite composite contains functional groups from CS and bentonite, which is beneficial to the adsorption of TC.

Figure 4 shows the TG-DTG curves for sodium-modified bentonite (a) and CS-modified bentonite (1:5) (b). the TG curve is a graph of the change in adsorbent mass with increasing temperature, and the DTG curve is a graph of the rate of change in the adsorbent mass with increasing temperature. As seen in Figure 4a, there are three mass loss processes in sodium-modified bentonite; the temperature increases from 30 to 125 °C, and the mass loss of sodium-modified bentonite is 1.37%, corresponding to the first strong heat absorption peak of the DTG curve, which is related to the loss of water molecules physically adsorbed by sodium-modified bentonite.[36] The 300−500 °C interval has a weaker heat absorption peak, and the mass loss in this interval is 0.61%, which is related to the loss of water molecules physically adsorbed by sodium-modified bentonite.[20] There is a second strong heat absorption peak between 500 and 700 °C, with a mass loss of 3.75% in this temperature interval, which is caused by the loss of structural water from sodium-modified bentonite, where dehydroxylation leads to the collapse of the internal structure of bentonite and the destruction of the adsorption properties.[36] As seen in Figure 4b, CS-modified bentonite has the first strong heat absorption peak in the interval from 30 to 200 °C. The mass loss in this interval is 4.86%, which is related to the loss of adsorbed water from CS-modified bentonite. There is a broad absorption peak at 200−400 °C with a mass loss of 1.69%, which is related to the decomposition of CS into CO_2, CO, and H_2O.[27] There is a second broad absorption peak at 400−700 °C with a mass loss of 3.09%, which is related to the loss of water from the structure of CS-modified bentonite. From the TG curve, it can be seen that the weight loss of CS-modified bentonite is significantly higher than that of sodium-modified bentonite, which proves that CS successfully combined with sodium-modified bentonite during the modification process, which is consistent with other characterization results.[36] At the same time, the rate of free water removal from the CS-modified bentonite adsorbent is the fastest, indicating that CS modification enhances the hydrophobicity of sodium-modified bentonite, which is beneficial to the practical application of CS-modified bentonite.

The nitrogen adsorption−desorption isotherms of sodium-modified bentonite and CS-modified bentonite are shown in Table 1. The Brunauer−Emmett−Teller (BET) specific surface areas (S_{BET}), total pore volumes, micropore volumes, and the average pore size of sodium-modified bentonite and CS-modified bentonite are listed in Table 1. The specific surface area of CS increased slightly after modification, while the pore volume and pore size were basically unchanged. CS may enhance the adsorption performance mainly through chemical action.[20]

2.2. Factor Optimization for TC Removal. *2.2.1. Effect of Different CS/Bentonite Ratios.* The effect of varied mass ratios on the adsorption effect of CS-modified bentonite was examined in this experiment. For static adsorption studies with TC, six adsorbents with CS bentonite mass ratios of 0:1, 1:1, 1:5, 1:10, 1:25, and 1:50 were performed, and the results are presented in Figure 5.

https://doi.org/10.1021/acsomega.3c00745
ACS Omega 2023, 8, 19455−19463

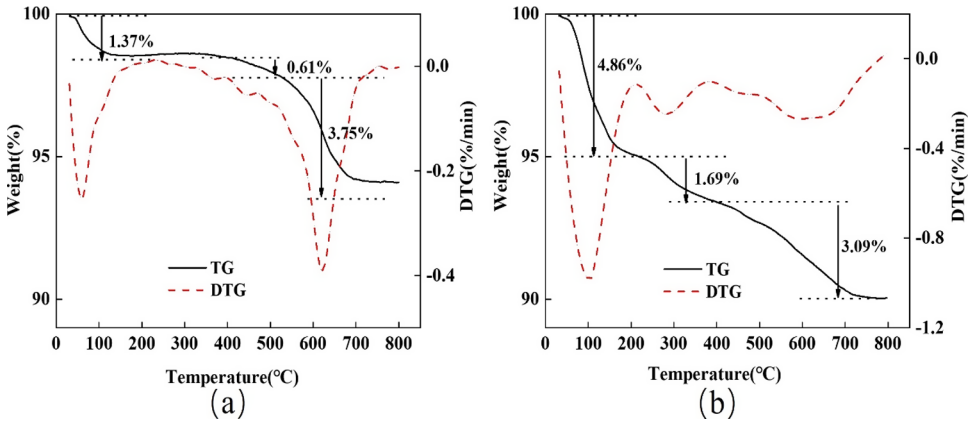

Figure 4. TG-DTG diagram of (a) sodium-modified bentonite and (b) CS-modified bentonite (1:5).

Table 1. Structural Information of Sodium-Modified Bentonite and CS-Modified Bentonite

adsorbents	S_{BET} (m^2/g)	pore volumes (cm^3/g)	pore size (nm)
sodium-modified bentonite	75.66	0.216	11.43
CS-modified bentonite	77.42	0.219	11.29

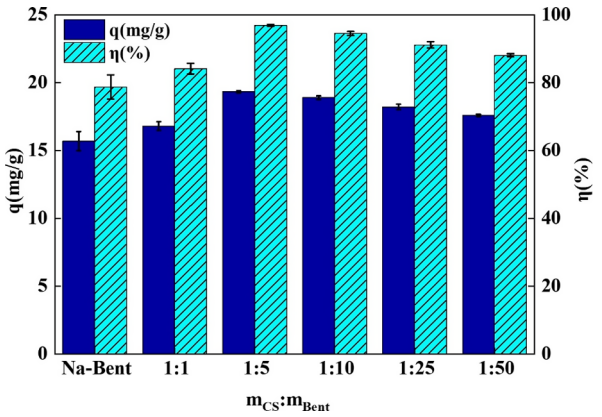

Figure 5. Effects of different mass ratios of CS and bentonite on adsorption of TC by CS-modified bentonite.

The adsorption effect of the five various mass ratios of CS-modified bentonite was greatly enhanced when compared to sodium-modified bentonite, as shown in Figure 5. The adsorption effect of CS-modified bentonite on TC steadily increased as the CS/bentonite mass ratio increased. The best adsorption result was obtained when the mass ratio was 1:5, with an adsorption capacity of 19.32 mg/g and a removal efficiency of 96.83%. When the mass ratio was raised to 1:1, the adsorption effectiveness was reduced. This might be because excess CS will cover the surface of bentonite and block the pore channels on the surface, impairing the mass transfer process of TC in solution and therefore the adsorption efficiency.[37] As a result, a mass ratio of 1:5 CS/bentonite was chosen for the following adsorbent preparation.

2.2.2. Effect of the Dosage of Adsorbents. The effect of different adsorbent dosages on the adsorption effect of TC by CS-modified bentonite was investigated in this experiment, and six gradients of 1, 2, 3, 5, 7, and 10 g/L were set for static adsorption experiments of TC, and the results are shown in Figure 6.

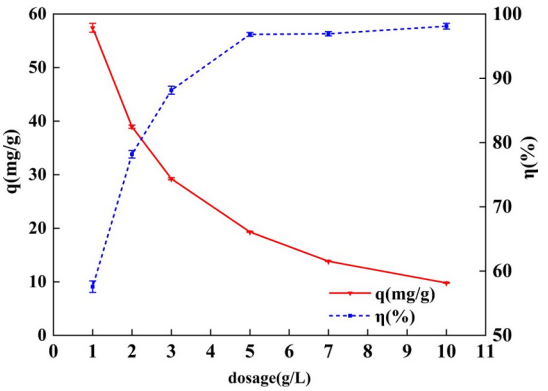

Figure 6. Effect of different dosages on adsorption of TC by CS-modified bentonite.

As shown in Figure 6, the TC adsorption capacity of CS-modified bentonite steadily declined with an increasing adsorbent dose, from 57.43 to 9.80 mg/g, and the change in adsorption capacity tended to stabilize. TC removal efficiency steadily improved from 57.43 to 98.11%, and subsequently the change in the removal rate stabilized. When the dosage was increased to 5 g/L, the CS-modified bentonite adsorption capacity for TC was 19.32 mg/g, and the removal efficiency was 96.83%. Further increases in dosage did not significantly enhance TC removal; hence, the adsorbent dosage for following tests was set at 5 g/L. Because the initial concentration of TC-simulated wastewater was the same in each adsorption experiment, there was a relative excess of TC in the solution at the lower adsorbent dosage.[38] The free adsorption sites on the surface of CS-modified bentonite could quickly bind to TC and reach adsorption saturation, resulting in a high adsorption capacity when the adsorbent dosage was low.[30] When the adsorbent dosage was increased to a certain extent, the amount of TC adsorbed on the adsorbent surface was higher than the total amount of TC in the solution, resulting in insufficient TC in the solution to occupy all the adsorption sites, and the adsorbent's adsorption capacity gradually decreased while the removal efficiency gradually increased.[10]

2.2.3. Effect of pH. The effect of varied initial pH values of TC-simulated wastewater on the effect of CS-modified bentonite on TC adsorption was studied in this experiment. For static adsorption experiments of TC, nine gradients of

https://doi.org/10.1021/acsomega.3c00745
ACS Omega 2023, 8, 19455−19463

starting pH (2, 3, 4, 5, 6, 7, 8, 9, and 10) were applied. The results are presented in Figure 7.

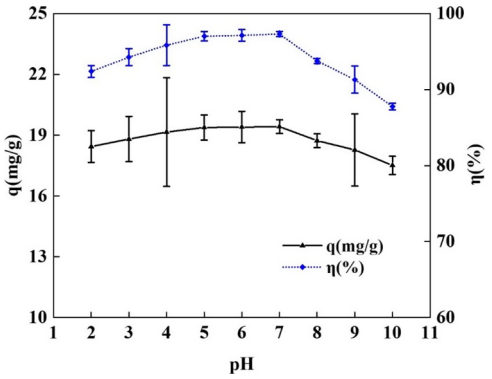

Figure 7. Effect of different initial pH values on adsorption of TC by CS-modified bentonite.

As can be seen from Figure 7, the adsorption capacity and removal efficiency of CS-modified bentonite for TC increased gradually with the gradual increase of pH under acidic conditions. Under neutral conditions, the adsorption capacity and removal efficiency of the adsorbent were the highest, reaching 96.83%. Under alkaline conditions, the adsorption capacity and removal efficiency gradually decreased. However, the overall removal efficiency remained above 85%, indicating that CS-modified bentonite had a wide pH range for the adsorption of TC.

2.2.4. Effect of Adsorption Time. In this experiment, the effect of different adsorption durations on the adsorption of TC by CS-modified bentonite was investigated. Eight temporal gradients from 5 to 120 min (5, 10, 20, 30, 45, 60, 90, and 120 min) were set for static adsorption of TC, and the results are shown in Figure 8.

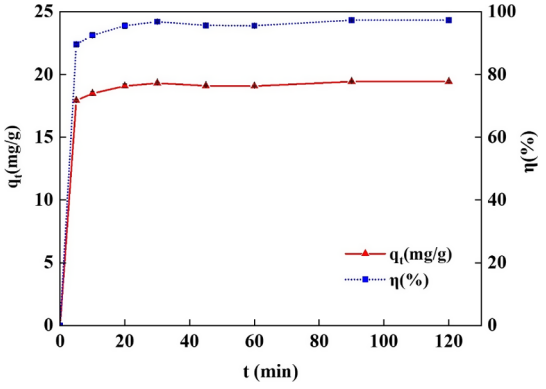

Figure 8. Effect of different adsorption times on adsorption of TC by CS-modified bentonite.

Figure 8 shows that during the first 5 min of adsorption, the adsorbent's TC adsorption capacity and removal efficiency both increased quickly, reaching 17.92 mg/g and 89.63%, respectively. TC's adsorption capacity and extraction efficiency reached equilibrium after 30 min, with a capacity of 19.32 mg/g and a removal efficiency of 96.83%. The adsorbent's removal effectiveness and capacity for adsorption did not vary appreciably throughout the course of the 30−120 min period. This was because there were a lot of free adsorption sites on the adsorbent surface at the beginning of the adsorption, which could quickly bind to the TC molecules in the solution, increasing the adsorption capacity and removal effectiveness.[39] The number of free adsorption sites on the adsorbent surface rapidly decreased as the adsorption period was prolonged, which reduced the adsorbent's ability to bind to the TC molecules. Adsorption equilibrium was ultimately established at 30 min. TC's adsorption capacity and removal efficiency were essentially unaffected even when the adsorption duration was prolonged.

In this study, the adsorption capacity was 19.32 mg/g under optimal conditions. Comparing to the similar CS/bentonite composites in other studies, this is higher than an adsorption capacity of 4.24 mg/g reported in the study of Turan et al.[40] CS altered montmorillonite was prepared by Ma et al.[41] and can be utilized for TC adsorption. The maximum adsorption capacity reached 42.45 mg/g during 4 h. However, the better adsorption capacity needs longer adsorption duration and an acidic environment (pH = 4). As a result, CS-modified bentonite synthesized in this study has better adsorption capacity and application prospect.

2.3. Adsorption Isotherms and Kinetics. *2.3.1. Adsorption Kinetics.* The kinetic simulation of the adsorption of TC by CS-modified bentonite was carried out using the pseudo-first-order kinetic model, pseudo-second-order kinetic model, Elovich model, and intraparticle diffusion model. The fitted results are shown in Figure 9 and the relevant parameters are shown in Table 2.

Table 2 shows that the correlation coefficients for the pseudo-first-order kinetic model and the pseudo-second-order kinetic model, both of which had a high fitting degree, were 0.998 and 0.999, respectively. It was discovered that the value derived using the pseudo-second-order kinetic model was closer to the measured value of 19.44 mg/g by comparing the fitted equilibrium adsorption capacity. This shows that the reaction mechanism is a chemisorption process with a rate constant of 0.119 $g \cdot mg^{-1} \cdot min^{-1}$ and that the pseudo-second-order kinetic model can better explain the adsorption of TC by CS-modified bentonite. The Elovich model's correlation coefficient was 0.999, and its high fitting degree shows that the reaction process is a nonhomogeneous diffusion process.[42] Figure 9d shows that the intraparticle diffusion model's fitted curve does not pass through the origin and that the fitted correlation coefficient is only 0.624, demonstrating that intraparticle diffusion is not the only rate-limiting step in the adsorption process and that a variety of factors interact to control the rate of the process.[43]

2.3.2. Adsorption Isotherms. For the TC static adsorption studies, three temperature gradients (20, 30, and 40 °C) and eight concentration gradients (50, 100, 150, 200, 300, 400, 500, and 600 mg/L) were set for each temperature. The results are reported in Table 3. As the initial concentration of TC-simulated wastewater increased, the increase in adsorption capacity (q_e) at the same temperature dropped. Indicating that the adsorption sites on the surface of the adsorbent were nearly saturated at this point and no more TC could be adsorbed, the concentration of TC in solution (C_e) progressively increased as the adsorption achieved equilibrium. The equilibrium adsorption capacity of the adsorbent steadily increased with rising temperature at the same initial concentration, showing that the rise in temperature was advantageous for adsorption to proceed.

The experimental data were fitted with the Langmuir model and Freundlich model, respectively, and the fitted results and

https://doi.org/10.1021/acsomega.3c00745
ACS Omega 2023, 8, 19455−19463

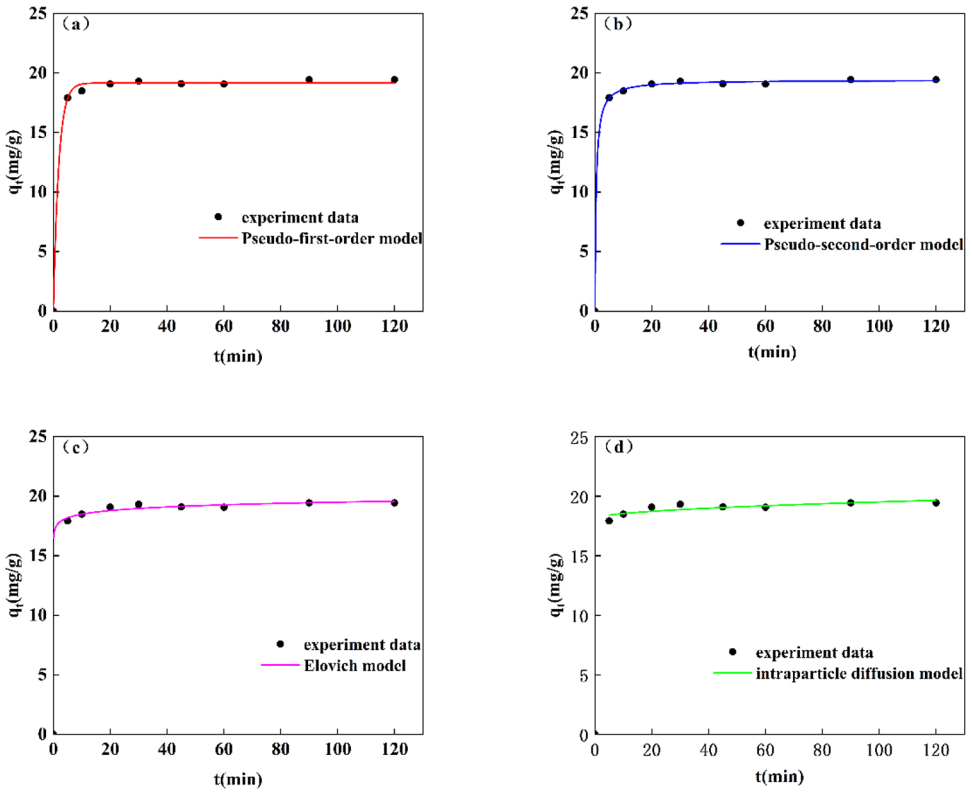

Figure 9. (a) Pseudo-first-order kinetic model, (b) pseudo-second-order kinetic model, (c) Elovich model, and (d) intraparticle diffusion model.

Table 2. Parameters of the Adsorption Kinetic Model

model	parameters		
pseudo-first-order kinetic model	q_e (mg/g)	K_1 (1/min)	R^2
	19.16	0.536	0.998
pseudo-second-order kinetic model	q_e (mg/g)	K_2 (g·mg^{-1}·min^{-1})	R^2
	19.42	0.119	0.999
Elovich model	β (mg/g)	ln($\alpha\beta$) (mg/g)	R^2
	2.29	39.95	0.999
intraparticle diffusion model	C (mg/g)	K_{ip} (mg·g^{-1}·min$^{-0.5}$)	R^2
	18.09	0.142	0.624

Table 3. q_e and C_e at Different Temperatures and Initial Concentrations

	20 °C (293 K)		30 °C (303 K)		40 °C (313 K)	
C_0 (mg/L)	q_e (mg/g)	C_e (mg/L)	q_e (mg/g)	C_e (mg/L)	q_e (mg/g)	C_e (mg/L)
50	9.72	1.34	9.81	0.85	9.93	0.26
100	19.13	4.25	19.44	2.68	19.67	1.59
150	28.29	8.59	28.44	7.51	29.22	3.56
200	37.00	14.61	37.44	12.24	38.39	7.9
300	53.15	34.14	54.54	27.13	56.53	17.17
400	69.02	54.25	71.28	43.11	74.08	28.32
500	83.23	82.95	87.38	62.24	91.62	41.53
600	95.90	119.74	97.49	112.14	103.38	82.56

parameters are shown in Figure 10 and Table 4. The fitted correlation coefficients of the Freundlich model at different temperatures were higher than those of the Langmuir model, and the adsorption process of TC by CS-modified bentonite was more consistent with the Freundlich model. This indicates that the adsorption process of TC by CS-modified bentonite is nonmonolayer adsorption, and TC is first adsorbed at the adsorption site that is easier to bind.[44] The $1/n$ values of the Freundlich model at different temperatures were less than 0.5, indicating that the reaction process was easier to carry out.[26]

2.3.3. Thermodynamic Analysis. By linearly fitting a graph of q_e with $\ln(q_e/C_e)$, the y-axis intercept, which is the thermodynamic equilibrium constant K_d at different temperatures, is obtained. Linear fitting output the following linear equations at different temperatures: $y = -0.0243 - x + 1.96$ (293 K), $y = -0.0257 - x + 2.34$ (303 K), and $y = -0.0298 - x + 3.20$ (303 K) (313 K). The Gibbs Helmholtz equation ($\Delta G^\theta = -RT \ln K_d$) was used to calculate ΔG^θ, which was then fitted linearly to ΔH^θ and ΔS^θ using the Van't Hoff equation $\left(\ln K_d = \frac{\Delta S^\theta}{R} - \frac{\Delta H^\theta}{RT}\right)$, with $\ln(K_d)$ plotted against $1/T$. Table 5 displays the relevant thermodynamic parameters.

The reaction of TC adsorption by CS-modified bentonite is a heat absorption process, as shown by the positive enthalpy change of the adsorption process (H = 18.71 kJ/mol) based on the thermodynamic parameters in Table 5. The adsorption process' entropy change (S = 69.26 J/mol) was positive, indicating that it is an entropy-increasing process and that the adsorption system is moving toward increasing confusion.[24] TC is adsorbing by the adsorbent at different temperatures, and the negative values of the Gibbs free energy (G = −1.64, −2.14, and −3.03 kJ/mol) show that the reaction can happen spontaneously. In light of the fact that TC adsorption by CS-modified bentonite is a spontaneous, heat-absorbing, entropy-increasing reaction process, raising the temperature is beneficial to the adsorption process.

https://doi.org/10.1021/acsomega.3c00745
ACS Omega 2023, 8, 19455−19463

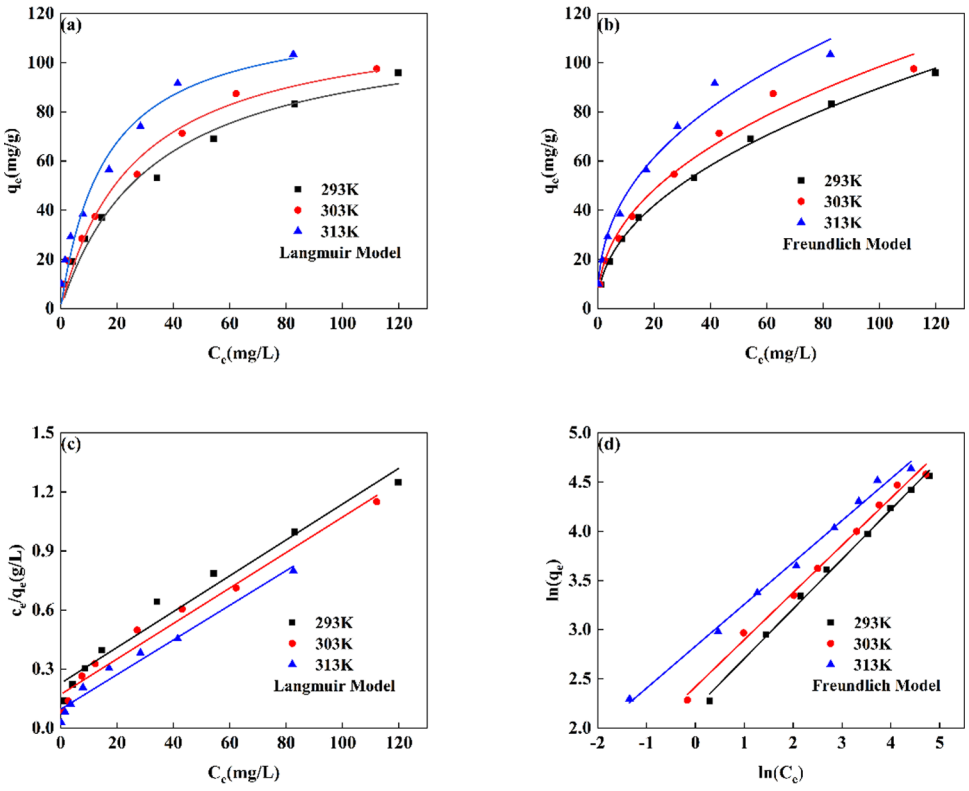

Figure 10. (a) Langmuir model, (b) Freundlich model, (c) linear fitting of the Langmuir model, and (d) linear fitting of the Freundlich model.

Table 4. Relevant Parameters of the Langmuir Model and the Freundlich Model

	Langmuir model			Freundlich model		
temperature (K)	q_m (mg/g)	K_L (L/mg)	R^2	K_F (mg/g)	$1/n$	R^2
293	116.40	0.0305	0.974	10.14	0.473	0.998
303	119.46	0.0377	0.973	12.85	0.442	0.981
313	121.36	0.0629	0.963	18.02	0.409	0.979

Table 5. Thermodynamic Parameters

temperature (K)	ΔG^θ (kJ/mol)	ΔH^θ (kJ/mol)	ΔS^θ (J/mol)
293	−1.64	18.71	69.26
303	−2.14		
313	−3.03		

3. CONCLUSIONS

In this study, a particular type of CS-modified bentonite was developed by the coprecipitation method and used to remove TC from wastewater. SEM, XRD, FTIR, TG, and BET characterization were used to investigate the physicochemical properties of the powder adsorbents. The adsorption process was more consistent with the Freundlich model and the pseudo-second-order kinetic model, indicating that it was a nonmonolayer chemisorption process. The adsorption process is a spontaneous, endothermic, entropy-increasing process, according to thermodynamic characteristics. In conclusion, it has been discovered that CS-modified bentonite has a high adsorption capacity and may be utilized to effectively remove TC from wastewater.

4. MATERIALS AND METHODS

4.1. Synthesis of CS-Modified Bentonite. *4.1.1. Purification of Bentonite.* The purification of bentonite is carried out by gravity sedimentation.[45,46] First, raw bentonite was put into a draught drying cabinet and dried at 105 °C for 2 h, then removed and cooled to room temperature, crushed using a ball mill to obtain the raw bentonite powder, and sealed in a bag and placed in a desiccator for storage. One hundred grams of raw bentonite powder was mixed with deionized water to make a 10% bentonite slurry, which was stirred vigorously for 30 min using a magnetic stirrer to disperse fully and left for 30 min. The upper layer of the slurry was taken and centrifuged for 10 min (1500 rpm), and the upper layer was poured off and the lower layer was dried in an oven at 105 °C for 24 h. Finally, the solid was crushed and passed through a 200 mesh sieve to obtain the purified bentonite powder.

4.1.2. Synthesis of Sodium-Modified Bentonite. The sodium modification of bentonite was carried out by the suspension method.[47] One hundred grams of purified bentonite powder was first prepared by adding deionized water to form a 10% slurry, which was stirred vigorously with a magnetic stirrer to disperse the bentonite powder, then 4 g of Na_2CO_3 was added and stirred for 90 min at 80 °C. After the slurry had cooled to room temperature, it was transferred to a centrifuge tube and separated by centrifugation at 1500 rpm for 10 min. The bottom solid obtained by centrifugation was dried in an oven at 105 °C for 24 h and then crushed and passed through a 200 mesh sieve to obtain sodium-modified bentonite.

4.1.3. Synthesis of CS-Modified Bentonite. To dissolve CS, 1.0 g was weighed into 200 mL of 5% acetic acid solution and vigorously stirred for 2 h at 60 °C. When the CS is entirely dissolved, a specified amount of sodium-modified bentonite

https://doi.org/10.1021/acsomega.3c00745
ACS Omega 2023, 8, 19455−19463

powder was added and thoroughly mixed it in. The reaction is filtered after 120 min of stirring, and the filter cake is washed with deionized water until the filtrate is neutral. To get CS-modified bentonite, the filter cake was dried in a vacuum drying oven at 60 °C for 24 h, crushed, and passed through a 200 mesh sieve.[48]

4.2. Material Characterization. The morphologies of the adsorbents were observed by Hitachi SU8200 scanning electron microscope. XRD patterns were collected in the 2θ range of 5−90° at a scan speed of 10°/min with CuKα radiation (Cu Kα,λ = 0.15406 nm, pipe voltage 40 kV, pipe current 40 mA) (D8 ADVANCE, Bruker, Germany). FTIR spectra were measured by using a Vertex 70v FTIR spectrophotometer. The FTIR tests were performed in a range of 400−4000 cm^{-1}. Thermogravimetric analysis was carried out using a thermogravimetric analyzer (TGA-50H, Shimadzu, Japan). Surface area and pore size distribution were measured by N_2 adsorption/desorption at 100 °C by an ASAP 2460 analyzer (Micromeritics Corporation, USA). The specific surface area and pore size distribution of samples were calculated by the BET equation and the Barrett−Joyner−Halenda (BJH) method, respectively.

4.3. Adsorption Experiments. In this study, adsorption experiments were carried with a controlled temperature of 25 °C and constant stirring (120 rpm). In each experiment, 50 mL of TC solution (100 mg L^{-1}) and 0.25 g of the adsorbent were used under different factorial design conditions. The supernatants were centrifuged and saved for measurement. Each solution's concentration was determined in a UV−vis spectrophotometer at a wavelength of 357 nm using the Lambert−Beer law. The equilibrium adsorption capacity (q_e, mg/g) and removal capacity (η %) was determined according to eqs 2 and 3.[49]

$$q = (C - C_0) \times \frac{V}{m} \tag{2}$$

$$\eta = \frac{C_0 - C}{C_0} \times 100\% \tag{3}$$

where q_e is the equilibrium adsorption capacity, C_0 is the initial concentration, C_e is the final concentration of TC in the solution, V is the volume of the aqueous solution in flasks, and m the mass of adsorbent used.

AUTHOR INFORMATION

Corresponding Author

Zhenjun Wu − *School of Environmental Engineering, Henan University of Technology, Zhengzhou 450001, China; Henan Xinanli Security Technology Co., Ltd. Post-Doctoral Workstation, Zhengzhou 450001, China;* orcid.org/0000-0002-0341-8977; Email: wuzhenjun@haut.edu.cn

Authors

Xuebai Guo − *Henan Vocational College of Water Conservancy and Environment, Zhengzhou 450008, China*

Zelong Wang − *School of Ecology and Environment, Zhengzhou University, Zhengzhou 450001, China*

Fangfang Lin − *Henan Institute of Metrology, Zhengzhou 450008, China*

Penghui Li − *School of Environmental Engineering, Henan University of Technology, Zhengzhou 450001, China*

Jiaxin Liu − *School of Environmental Engineering, Henan University of Technology, Zhengzhou 450001, China*

Complete contact information is available at: https://pubs.acs.org/10.1021/acsomega.3c00745

Notes

The authors declare no competing financial interest.

ACKNOWLEDGMENTS

This work was supported by the Key Research and Development Project of Henan Province (212102310070 and 232102320099), Natural Science Foundation of Henan (202300410107), Science and Technology Key Project Foundation of Henan Provincial Education Department (21B610005), and Doctoral Scientific Fund Project of Henan University of Technology (2019BS038).

REFERENCES

(1) Liu, C.; Tan, L.; Zhang, L.; Tian, W.; Ma, L. A Review of the Distribution of Antibiotics in Water in Different Regions of China and Current Antibiotic Degradation Pathways. *Front. Environ. Sci.* **2021**, *9*, No. 692298.

(2) Xu, L. S.; Wang, W. Z.; Deng, J. B.; Xu, W. H. The Residue of Tetracycline Antibiotics in Soil and Brassica Juncea Var. Gemmifera, and the Diversity of Soil Bacterial Community under Different Livestock Manure Treatments. *Environ. Geochem. Health* **2023**, *45*, 7−17.

(3) Frascaroli, G.; Reid, D.; Hunter, C.; Roberts, J.; Helwig, K.; Spencer, J.; Escudero, A. Pharmaceuticals in Wastewater Treatment Plants: A Systematic Review on the Substances of Greatest Concern Responsible for the Development of Antimicrobial Resistance. *Appl. Sci.* **2021**, *11*, 6670.

(4) Tetracycline antibiotics in the environment: a review | SpringerLink. https://link.springer.com/article/10.1007/s10311-013-0404-8 (accessed February 2023).

(5) Ahmadi, M.; Motlagh, H. R.; Jaafarzadeh, N.; Mostoufi, A.; Saeedi, R.; Barzegar, G.; Jorfi, S. Enhanced Photocatalytic Degradation of Tetracycline and Real Pharmaceutical Wastewater Using MWCNT/TiO2 Nano-Composite. *J. Environ. Manage.* **2017**, *186*, 55−63.

(6) Liao, Q.; Rong, H.; Zhao, M.; Luo, H.; Chu, Z.; Wang, R. Interaction between Tetracycline and Microorganisms during Wastewater Treatment: A Review. *Sci. Total Environ.* **2021**, *757*, No. 143981.

(7) Fan, B.; Tan, Y.; Wang, J.; Zhang, B.; Peng, Y.; Yuan, C.; Guan, C.; Gao, X.; Cui, S. Application of Magnetic Composites in Removal of Tetracycline through Adsorption and Advanced Oxidation Processes (AOPs): A Review. *Processes* **2021**, *9*, 1644.

(8) Wang, T.; Xue, L.; Liu, Y.; Fang, T.; Zhang, L.; Xing, B. Insight into the Significant Contribution of Intrinsic Defects of Carbon-Based Materials for the Efficient Removal of Tetracycline Antibiotics. *Chem. Eng. J.* **2022**, *435*, No. 134822.

(9) Kong, Y.; Han, K.; Zhuang, Y.; Shi, B. Facile Synthesis of MOFs-Templated Carbon Aerogels with Enhanced Tetracycline Adsorption Performance. *Water* **2022**, *14*, 504.

(10) Ortiz-Ramos, U.; Leyva-Ramos, R.; Mendoza-Mendoza, E.; Aragon-Pina, A. Removal of Tetracycline from Aqueous Solutions by Adsorption on Raw Ca-Bentonite. Effect of Operating Conditions and Adsorption Mechanism. *Chem. Eng. J.* **2022**, *432*, No. 134428.

(11) Wu, Y.; Yang, M.; Long, D.; Yang, F.; Luo, S. Tetracycline Adsorption on Magnetic Sludge Biochar: Effects of PH, Humic Acid (HA), and Fulvic Acid (FA). *Micromachines* **2022**, *13*, 1057.

(12) Xia, C.; Huang, H.; Liang, D.; Xie, Y.; Kong, F.; Yang, Q.; Fu, J.; Dou, Z.; Zhang, Q.; Meng, Z. Adsorption of Tetracycline Hydrochloride on Layered Double Hydroxide Loaded Carbon Nanotubes and Site Energy Distribution Analysis. *Chem. Eng. J.* **2022**, *443*, No. 136398.

(13) Bruckmann, F. d. S.; Ledur, C. M.; da Silva, I. Z.; Dotto, G. L.; Bohn Rhoden, C. R. A DFT Theoretical and Experimental Study

about Tetracycline Adsorption onto Magnetic Graphene Oxide. *J. Mol. Liq.* **2022**, *353*, No. 118837.
(14) Gopal, G.; Alex, S. A.; Chandrasekaran, N.; Mukherjee, A. A Review on Tetracycline Removal from Aqueous Systems by Advanced Treatment Techniques. *RSC Adv.* **2020**, *10*, 27081−27095.
(15) Pandey, S. A Comprehensive Review on Recent Developments in Bentonite-Based Materials Used as Adsorbents for Wastewater Treatment. *J. Mol. Liq.* **2017**, *241*, 1091−1113.
(16) Shen, Q.; Xu, M.-H.; Wu, T.; Pan, G.-X.; Tang, P.-S. Adsorption Behavior of Tetracycline on Carboxymethyl Starch Grafted Magnetic Bentonite. *Chem. Pap.* **2022**, *76*, 123−135.
(17) Huang, Z.; Li, Y.; Chen, W.; Shi, J.; Zhang, N.; Wang, X.; Li, Z.; Gao, L.; Zhang, Y. Modified Bentonite Adsorption of Organic Pollutants of Dye Wastewater. *Mater. Chem. Phys.* **2017**, *202*, 266.
(18) Wang, Y.; Jiang, Q.; Cheng, J.; Pan, Y.; Yang, G.; Liu, Y.; Wang, L.; Leng, Y.; Tuo, X. Synthesis and Characterization of CTAB-Modified Bentonite Composites for the Removal of Cs+. *J. Radioanal. Nucl. Chem.* **2021**, *329*, 451−461.
(19) Jin, X.; Zheng, M.; Sarkar, B.; Naidu, R.; Chen, Z. Characterization of Bentonite Modified with Humic Acid for the Removal of Cu (II) and 2,4-Dichlorophenol from Aqueous Solution. *Appl. Clay Sci.* **2016**, *134*, 89−94.
(20) Berraaouan, D.; Elmiz, M.; Essifi, K.; Salhi, S.; Tahani, A. Adsorption of Carvacrol on Modified Bentonite in Aqueous Solutions. *Mater. Today: Proc.* **2020**, *31*, S28−S32.
(21) Olafadehan, O. A.; Bello, V. E.; Amoo, K. O. Production and Characterization of Composite Nanoparticles Derived from Chitosan. CTAB and Bentonite Clay. *Chem. Pap.* **2022**, *76*, 5063−5086.
(22) Zhou, F.; Li, J.; Zhou, L.; Liu, Y. Preparation and Mechanism of a New Enhanced Flocculant Based on Bentonite for Drinking Water. *Adv. Mater. Sci. Eng.* **2015**, *2015*, No. 579513.
(23) Wang, Z.; Muhammad, Y.; Tang, R.; Lu, C.; Yu, S.; Song, R.; Tong, Z.; Han, B.; Zhang, H. Dually Organic Modified Bentonite with Enhanced Adsorption and Desorption of Tetracycline and Ciprofloxacine. *Sep. Purif. Technol.* **2021**, *274*, No. 119059.
(24) Wu, Z.; Li, S.; Wan, J.; Wang, Y. Cr(VI) Adsorption on an Improved Synthesised Cross-Linked Chitosan Resin. *J. Mol. Liq.* **2012**, *170*, 25−29.
(25) Bruckmann, F. d. S.; Schnorr, C. E.; Salles, T. d. R.; Nunes, F. B.; Baumann, L.; Mueller, E. I.; Silva, L. F. O.; Dotto, G. L.; Bohn Rhoden, C. R. Highly Efficient Adsorption of Tetracycline Using Chitosan-Based Magnetic Adsorbent. *Polymer* **2022**, *14*, 4854.
(26) Huang, R.; Yang, B.; Wang, B.; Zheng, D.; Zhang, Z. Removal of Chromium (VI) Ions from Aqueous Solutions by N-2-Hydroxypropyl Trimethyl Ammonium Chloride Chitosan-Bentonite. *Desalin. Water Treat.* **2012**, *50*, 329−337.
(27) Perez, J. J.; Villanueva, M. E.; Sánchez, L.; Ollier, R.; Alvarez, V.; Copello, G. J. Low Cost and Regenerable Composites Based on Chitin/Bentonite for the Adsorption Potential Emerging Pollutants. *Appl. Clay Sci.* **2020**, *194*, No. 105703.
(28) Yang, J.; Huang, B.; Lin, M. Adsorption of Hexavalent Chromium from Aqueous Solution by a Chitosan/Bentonite Composite: Isotherm, Kinetics, and Thermodynamics Studies. *J. Chem. Eng. Data* **2020**, *65*, 2751−2763.
(29) Yadi, M. G.; Benguella, B.; Gaouar-Benyelles, N.; Tizaoui, K. Adsorption of Ammonia from Wastewater Using Low-Cost Bentonite/Chitosan Beads. *Desalin. Water Treat.* **2016**, *57*, 21444−21454.
(30) Laysandra, L.; Ondang, I. J.; Ju, Y.-H.; Ariandini, B. H.; Mariska, A.; Soetaredjo, F. E.; Putro, J. N.; Santoso, S. P.; Darsono, F. L.; Ismadji, S. Highly Adsorptive Chitosan/Saponin-Bentonite Composite Film for Removal of Methyl Orange and Cr(VI). *Environ. Sci. Pollut. Res. Int.* **2019**, *26*, 5020−5037.
(31) Savitri, E.; Budhyantoro, A. The Effect of Ratio Chitosan-Bentonite and Processing Time on the Characterization of Chitosan-Bentonite Composite. *IOP Conf. Ser.: Mater. Sci. Eng.* **2017**, *223*, No. 012034.
(32) Mo, W.; He, Q.; Su, X.; Ma, S.; Feng, J.; He, Z. Preparation and Characterization of a Granular Bentonite Composite Adsorbent and Its Application for Pb2+ Adsorption. *Appl. Clay Sci.* **2018**, *159*, 68−73.
(33) Pawar, R. R.; Lalhmunsiama; Ingole, P. G.; Lee, S.-M. Use of Activated Bentonite-Alginate Composite Beads for Efficient Removal of Toxic Cu2+ and Pb2+ Ions from Aquatic Environment. *Int. J. Biol. Macromol.* **2020**, *164*, 3145−3154.
(34) Belhouchat, N.; Zaghouane-Boudiaf, H.; Viseras, C. Removal of Anionic and Cationic Dyes from Aqueous Solution with Activated Organo-Bentonite/Sodium Alginate Encapsulated Beads. *Appl. Clay Sci.* **2017**, *135*, 9−15.
(35) Liu, Q.; Huang, R.; Yang, B.; Liu, Y. Adsorption of Fluoride from Aqueous Solution by Enhanced Chitosan/Bentonite Composite. *Water Sci. Technol.* **2013**, *68*, 2074−2081.
(36) Kalburcu, T.; Tabak, A.; Ozturk, N.; Tuzmen, N.; Akgol, S.; Caglar, B.; Denizli, A. Adsorption of Lysozyme from Aqueous Solutions by a Novel Bentonite−Tyrptophane (Bent−Trp) Microcomposite Affinity Sorbent. *J. Mol. Struct.* **2015**, *1083*, 156−162.
(37) Bensalem, S.; Hamdi, B.; Del Confetto, S.; Calvet, R. Characterization of Surface Properties of Chitosan/Bentonite Composites Beads by Inverse Gas Chromatography. *Int. J. Biol. Macromol.* **2021**, *166*, 1448−1459.
(38) Li, S.; Wu, Z.; Li, B.; Zhu, R.; Wang, Y. Chitosan Resins Synthesised by Improved Drop-Sphere-Forming Method for Cr(VI) Removal from Aqueous Solutions. *Water Sci. Technol.* **2012**, *66*, 2461−2467.
(39) Fagundes, A. P.; da Silva, A. F. V.; de Morais, B. B.; Macuvele, D. L. P.; Nones, J.; Riella, H. G.; Padoin, N.; Soares, C. A Novel Application of Bentonite Modified with Copper Ions in the Tetracycline Adsorption: An Experimental Design Study. *Mater. Lett.* **2021**, *291*, No. 129552.
(40) Turan, B.; Sarigol, G.; Demircivi, P. Adsorption of Tetracycline Antibiotics Using Metal and Clay Embedded Cross-Linked Chitosan. *Mater. Chem. Phys.* **2022**, *279*, No. 125781.
(41) Ma, J.; Lei, Y.; Khan, M. A.; Wang, F.; Chu, Y.; Lei, W.; Xia, M.; Zhu, S. Adsorption Properties, Kinetics & Thermodynamics of Tetracycline on Carboxymethyl-Chitosan Reformed Montmorillonite. *Int. J. Biol. Macromol.* **2019**, *124*, 557−567.
(42) Song, H.; Gurav, R.; Bhatia, S.; Lee, E.; Kim, H. J.; Yang, Y.-H.; Kan, E.; Kim, H.; Lee, S. H.; Choi, Y.-K. Treatment of Microcystin-LR Cyanotoxin Contaminated Water Using Kentucky Bluegrass-Derived Biochar. *J. Water Proc. Eng.* **2021**, *41*, No. 102054.
(43) Wang, Y.; Gong, S.; Li, Y.; Li, Z.; Fu, J. Adsorptive Removal of Tetracycline by Sustainable Ceramsite Substrate from Bentonite/Red Mud/Pine Sawdust. *Sci. Rep.* **2020**, *10*, 2960.
(44) Chen, Y.-G.; Ye, W.-M.; Yang, X.-M.; Deng, F.-Y.; He, Y. Effect of Contact Time, PH, and Ionic Strength on Cd(II) Adsorption from Aqueous Solution onto Bentonite from Gaomiaozi, China. *Environ. Earth Sci.* **2011**, *64*, 329−336.
(45) Ismail, S. H.; Mabrouk, M. S.; Ali-Almotalib, A.; Abn-Elwalead, K. Synthesis and Characterization of Bentonite Nanocomposites from Egyptian Bentonite Clay. *Int. J. Nanotechnol. Allied Sci.* **2017**, *1*, 16−29.
(46) Gong, Z.; Liao, L.; Lv, G.; Wang, X. A Simple Method for Physical Purification of Bentonite. *Appl. Clay Sci.* **2016**, *119*, 294−300.
(47) Yang, D.; Cheng, F.; Chang, L.; Wu, D. Sodium Modification of Low Quality Natural Bentonite as Enhanced Lead Ion Adsorbent. *Colloids Surf., A* **2022**, *651*, No. 129753.
(48) Huang, R.; Liu, Q.; Zhang, L.; Yang, B. Utilization of Cross-Linked Chitosan/Bentonite Composite in the Removal of Methyl Orange from Aqueous Solution. *Water Sci. Technol.* **2015**, *71*, 174−182.
(49) Xu, X.; Cheng, Y.; Wu, X.; Fan, P.; Song, R. La(III)-Bentonite/Chitosan Composite: A New Type Adsorbent for Rapid Removal of Phosphate from Water Bodies. *Appl. Clay Sci.* **2020**, *190*, No. 105547.

https://doi.org/10.1021/acsomega.3c00745
ACS Omega 2023, 8, 19455−19463